Hindawi
Journal of Spectroscopy
Volume 2020, Article ID 9170412, 9 pages
https://doi.org/10.1155/2020/9170412

Research Article

A Study of Fluoride-Containing Bioglass System for Dental Materials Derived from Clam Shell and Soda Lime Silica Glass

Rohaniah Abdul Jalil,[1] Khamirul Amin Matori,[1,2] Mohd Hafiz Mohd Zaid,[1] Norhazlin Zainuddin,[3] Mohammad Zulhasif Ahmad Khiri,[2] Nadia Asyikin Abdul Rahman,[1] Wan Nurshamimi Wan Jusoh,[1] and Esra Kul[4]

[1]*Department of Physics, Faculty of Science, Universiti Putra Malaysia, 43400, Serdang, Selangor, Malaysia*
[2]*Material Synthesis and Characterization Laboratory, Institute of Advanced Technology, Universiti Putra Malaysia, 43400, Serdang, Selangor, Malaysia*
[3]*Department of Chemistry, Faculty of Science, Universiti Putra Malaysia, 43400, Serdang, Selangor, Malaysia*
[4]*Department of Prosthodontic, Faculty of Dentistry, Ataturk University, 25030 Erzurum, Turkey*

Correspondence should be addressed to Khamirul Amin Matori; khamirul@upm.edu.my

Received 5 November 2019; Revised 19 January 2020; Accepted 5 February 2020; Published 21 April 2020

Academic Editor: Hakan Arslan

Copyright © 2020 Rohaniah Abdul Jalil et al. This is an open access article distributed under the Creative Commons Attribution License, which permits unrestricted use, distribution, and reproduction in any medium, provided the original work is properly cited.

The alumino-silicate-fluoride (ASF) bioglass system with empirical formula $[(45\text{-}x)SiO_2\text{-}xCaF_2\text{-}20P_2O_5\text{-}20Al_2O_3\text{-}15CaO]$ where $x = 5$, 10, 15, and 20 (wt.%) has been synthesised by using conventional melt-quenching method. In this study, soda lime silica (SLS) glass and clam shell (CS) vitreous waste were utilized as a source of silicon dioxide (SiO_2) and calcium oxide (CaO), respectively. The different physical behaviors of ASF bioglass were closely related to the CaF_2 content in each composition. The structural analysis shows the presence of various chemical bonds showing the formation of ASF bioglass. The ASF bioglass has many applications in dental field and efforts to improve its formulation can promise a better future in medical procedures.

1. Introduction

Researchers are working hard to improve the formulation of medical products available in market to meet the needs of the public. With the best of knowledge, biomaterials play a main role in the field of biomedical, as they can interact well in biological system [1, 2]. Due to their unique features and wide range of applications, researchers work are still working to obtain better properties and performances of biomaterials in biomedical field [3, 4]. On the other hand, bioglass with good antimicrobial and mechanical properties has been the potential candidate for biomaterial formulation in orthopedic and dental applications [5, 6]. The influence of bioglass in biomedical has proven to solve many problems, especially in dental procedures [7].

Discovered in 1969 by Hench, 45S5 Bioglass® is an example of biomaterial that provides biological response to the human body through the interaction of their ionic dissolution products with the physiological environment [8, 9]. As an early generation of biomaterial, 45S5 Bioglass® consist of $45SiO_2\text{-}24.5Na_2O\text{-}24.4CaO\text{-}6P_2O_5$ (wt.%) glass composition [10]. This composition selection has shown bioactive properties of bioglass and high reactivity behavior at the surface of the material [1, 7]. The current clinical use of bioglass shows the formation of hydroxyapatite-like layer during implantation process with the biological system which provides stable adhesion to living tissue [11–13]. This proves that bioglass is one of the most successful innovations in the field of biomedical.

The alumino-silicate-fluoride (ASF) based bioglass containing fluoride is known to be one of the earliest being produced with $SiO_2\text{-}CaO\text{-}CaF_2\text{-}P_2O_5\text{-}Al_2O_3$ composition. The calcium fluoride (CaF_2) content has an influence on the physical, chemical, and therapeutic properties of bioactive

glass as it is composed of calcium ion (Ca^{2+}) and fluoride ion (F^{-}) [14]. Additionally, the fluoride ion of CaF_2 is specifically used to characterize glass behavior as it can alter the nature of glass material which contributes to its use in dental and medical field [15–17]. Moreover, fluoride ion plays a major role in the composition of glass as it can enhance the remineralization of biological system [18, 19]. Besides, fluoride acts as a vital component in which it can reduce the melting point of the bioglass system [20]. From previous studies, various nucleating agents had successfully promoted the crystallization process for glass and improved the formation of fine-grained structure [21, 22]. In this work, CaF_2 also acts as a nucleating agent for the ASF bioglass crystallization process.

The preparation of ASF bioglass by using pure SiO_2 and CaO is very expensive and requires a high melting point for glass synthesis. To counter the problem, recycled SLS glass and CS will provide SiO_2 and CaO sources where it can reduce the production cost of ASF bioglass [23]. The fabrication of ASF bioglass with composition of silica, aluminium, and fluoride in this study shows soda lime silica (SLS) glass and clam shell (CS) vitreous waste material have been selected to replace certain elements in bioglass composition [14]. Since the major chemical compositions of SLS glass are basically SiO_2 (60–75%) and CaO (5–12%), it can be used as a source of silica in ASF bioglass composition for dental applications [24]. In the field of conventional glasses, SLS is known as a basic commercial glass product containing 95–99% of the glass produced worldwide. Generally, SLS glass is used for utensil, bioactive materials, and building material industries [25, 26]. Besides, CS or their scientific name *Anadara granosa* also become a potential candidate in the preparation of dental application. The CS is widely found in intertidal mudflats area mostly in Southeast Asian countries including Malaysia. It became an alternative biomaterial for biomedical application due to the fact that it richly contains calcium carbonate ($CaCO_3$) [27, 28]. Both SLS glass and CS are expected to provide better mechanical and optical properties such as high thermal stability, high transparency, and low melting point.

To the best of our knowledge, the study of the preparation of ASF bioglass from vitreous waste materials is relatively new and very limited in biomedical field. In this work, the preparation of ASF bioglass from vitreous waste material has been reported. The main objective of this work is to synthesis ASF bioglass from vitreous waste material. The effects of CaF_2 in each sample were also studied. The glass has been characterized by studying their physical and structural properties including X-ray fluorescence (XRF), density (ρ), molar volume (V_m), X-ray diffraction (XRD), Fourier transform infrared spectroscopy (FTIR), field emission scanning electron microscopy (FESEM), and energy dispersive X-ray (EDX) spectroscopy. The main advantage of the CaO-SLS glass system over the CaO-SiO_2 glass system is that it can reduce the production cost of ASF bioglass. Therefore, the idea of this article is to synthesis and characterize the ASF bioglass derived from CaO-SLS glass system.

2. Materials and Methods

2.1. Materials. The raw chemical compound for bioglass synthesis, SiO_2, was replaced with SLS glass waste bottles obtained from local restaurant in Selangor, Malaysia. Meanwhile, CaO was obtained from Cockle Shell (CS) or their scientific name (*Anadara granosa* sp.) from mangrove forest in Pontian, Johor, in South Coast of Peninsular Malaysia. For other chemical compounds, aluminum oxide 99.5% (Alfa Aesar, a Johnson Matthey Company), phosphorus pentoxide >99.99% (Alfa Aesar, a Johnson Matthey Company), and calcium fluoride >99.95% (R&M Chemicals) were used for ASF bioglass composition.

2.2. Preparation of Raw Materials. For preparing samples, raw materials were categorised into two components which were waste and commercial. Starting with waste materials, SLS glass and CS replaced SiO_2 and CaO, respectively. First, the SLS glass was thoroughly washed with water to remove the impurities and left to dry at room temperature for 24 hours. After drying, the SLS glass bottle was crushed into smaller pieces by using a hammer and followed by a plunge using steel plunger to obtain fine glass powder. Subsequently, the SLS glass was inserted into a milling jar containing 15–25 milling balls for a milling process about 80 r.p.m. for 24 hours. Then, it was ground using mortar and pestle continuously followed by sieving below 45 μm grain siever size to obtain SLS glass powder. The purpose of using a 45 μm siever was to achieve the smallest particle size of powder. Then, the collected CS wastes were washed with water to remove all impurities and left to dry for 24 hours at room temperature. The CO_2 was released from main composition of CS which is $CaCO_3$ through calcination process at 900°C for 2 hours in LT098 model SIC4-1600 furnace to obtain the CaO compound. Then, the CS was crushed using a plunger followed by sieved process using a 45 μm siever. Next, ASF bioglass was produced from a mixture of all five chemical compounds CaO, SiO_2, CaF_2, Al_2O_3, and P_2O_5. Table 1 shows the compositions used in the preparation of Batches 1, 2, 3, and 4 of bioglass samples labeled as B1G, B2G, B3G, and B4G, respectively.

2.3. Preparation of ASF Bioglass. Four batches of ASF bioglass sample were weighed ~80.0 g for each mixture as shown in Table 1. The samples were weighed by using an electronic digital weighing machine. The electronic digital weighing machine can provide reading up to ±0.0001 g accuracy. After mixing process, the mixture was transferred to a milling jar using a US Stoneware Jar Mill NA model at a speed range of approximately 80 r.p.m. and milled for about 15 minutes to ensure that the powder was homogeneous. Then, homogeneous powder was mixed into the crucible and the mixture was melted in LT Furnace model with a temperature increase rate at 10°C per minute about 4 hours at 1500°C. After 4 hours, the mixture underwent a water quenching process where thermal shock occurs and glass frit was produced. The glass frits underwent a drying process at room temperature for 24 hours to ensure the water was

Table 1: The weight percentage (wt.%) of ASF bioglass composition.

Batch	B1G	B2G	B3G	B4G
Weight percentage (wt.%)				
CaF_2	5	10	15	20
SiO_2	40	35	30	25
CaO	15	15	15	15
P_2O_5	20	20	20	20
Al_2O_3	20	20	20	20
Total	100	100	100	100

completely removed. Subsequently, the glass frits were crushed and ground to obtain the powder form using plungers and hammers. The powder form was sieved using siever with size of 45 μm to produce a fine powder form. Bioglass samples were characterized to determine the properties of raw CS and SLS glass samples.

2.4. Characterization. Raw CS and SLS glass were characterized by XRF measurement while ASF bioglass samples were characterized by using density, molar volume, XRD, FTIR, FESEM, and EDX. The result for chemical composition of bioglass was determined by analysis technique fundamental parameters (theoretical) through XRF spectroscopy using an Energy Dispersive X-ray Fluorescence model EDX-720 Shimadzu. The density of bioglass was measured using the Archimedes principle in which distilled water acts as an immersion liquid. In order to obtain the density of bioglass sample (ρ_{sample}), the bioglass sample was weighed in the air (W_{air}), then the sample was immersed in distilled water (W_{water}). Meanwhile, the density of distilled water (ρ_{water}) used in this measurement was 1.00 g/cm^3:

$$\rho_{\text{sample}} = \frac{W_{\text{air}}}{W_{\text{air}} - W_{\text{water}}} \times \rho_{\text{water}}. \quad (1)$$

The molar volume of ASF bioglass sample (V_m) is obtainted through the following equation:

$$V_m = \frac{\sum M}{\rho} \times \rho_{\text{water}}. \quad (2)$$

The total molecular weight of the ASF bioglass sample is represented as (M) while the density of the ASF bioglass is represented as (ρ).

The XRD measurement was carried out at 20° to 80° angles. X-ray Phillips (model PW 1830) was used to identify the structure of ASF bioglass sample. The results obtained were analyzed using X'Pert Highscore software. FTIR characterization was used to determine the chemical bond of the sample. The sample was analyzed by UATR-FTIR (Universal Attenuated Total Internal Reflection Fourier Transform Infrared) spectra recorded using a Thermo Scientific Nicolet 6700 FT-IR spectrometer in the range of 2000–200 cm^{-1} in 4 cm^{-1} resolution. Then, FESEM analysis was measured on ASF bioglass coated using gold (Au) to detect the morphology of the glass structure by using a high vacuum FEI Nova NanoSEM 230. The gold (Au) coating may disrupt the element at 2.2 keV of energy and phosphorus (P) is a potential element that can overlap to a certain degree at 2.1–2.2 keV of energy [29, 30]. As a solution to the overlapping problem, EDX analysis was completed before the sample was coated with gold (Au). The ASF samples were coated with gold (Au) for FESEM to prevent the charging issues. Finally, EDX measurement was performed to analyze the elements present in each sample. Each of the samples also using FEI Nova NanoSEM 230 in high-resolution field emission SEM where it is the main imaging tool for nanoparticles, with a resolution of 1 nm at 15 kV. The identification of weight percentage of C, O, F, Na, Al, Si, P, and Ca was measured by quantitative analysis. The quantitative analysis was conducted by Instruments NanoAnalysis (INCA) microanalysis of system based on standardless analysis. The standardless analysis will detect the element by calculating the area covered by each element below the peak. The Ca/P ratio is calculated to obtain the sensitivity factor by converting the area of peak to weight percentage. The Ca/P ratio is obtained by considering each elemental weight percentage of Ca and P.

3. Results and Discussion

3.1. X-Ray Fluorescence (XRF). The SLS glass and CS known as vitreous waste materials were used in the synthesis of ASF bioglass. Both waste materials become a prime source for SiO_2 and CaO, respectively. The XRF chemical analysis of raw SLS, CS, and CS after calcination can be seen in Table 2. From the table, the main elements present in the SLS glass are Si and Ca. These elements contain about 79.09 wt.% and 18.10 wt.% of weight percentage from the total composition. Other minor elements such as Al, K, Ti, Cr, Fe, Zn, Sr, and Zr comprise about 2.81% of the total composition. The commercial SLS glass is fundamentally composed of SiO_2, CaO, Na_2O, Al_2O_3, P_2O_5, and other oxide elements [31]. High composition of SiO_2 in SLS glass show the potential in glass production as Si is a dominant element in the glass matrix. As a major element in SLS glass, silica becomes a great source of raw materials for glass production [23, 24].

Meanwhile, raw CS shows that Ca is the major element which is around 97.70 wt.% from the total composition. The minor elements present in the composition are Zn, K, Sc, S, Sr, and Cu which is about 2.30 wt.%. From the table, Ca is the major element after calcination which is around 99.55 wt.% while the minor elements present are Sr and Cu around 0.46 wt.%. The CS act as a major source for CaO where it contains high amounts of calcium carbonate ($CaCO_3$). From the calcination process, $CaCO_3$ will be converted into CaO through the chemical decomposition reaction [27, 32]:

$$CaCO_{3\,(\text{solid})} + \text{Heat} \longrightarrow CaO_{(\text{solid})} + CO_{2\,(\text{gas})} \quad (3)$$

Minor elements in CS are eliminated during calcination. The Ca^{2+} ions have small ionic radius which may generate stronger and shorter Ca–O bond. Therefore as a final product of calcination process, CaO act as an oxide modifier which can increase the durability of glass production [33].

3.2. Density and Molar Volume. Figure 1 shows the graph of the density and molar volume for different ASF bioglass

Table 2: Chemical composition by XRF analysis of raw SLS, CS, and CS after calcination.

Element	Concentration%		
	Raw SLS	Raw CS	CS after calcination
Calcium, Ca	18.10	97.70	99.55
Strontium, Sr	0.25	0.27	0.34
Potassium, K	0.87	0.47	—
Zinc, Zn	0.038	0.67	—
Aluminium, Al	0.58	—	—
Silica, Si	79.09	—	—
Titanium, Ti	0.46	—	—
Chromium, Cr	0.033	—	—
Iron, Fe	0.42	—	—
Zirconium, Zr	0.17	—	—
Scandium, Sc	—	0.36	—
Sulfur, S	—	0.31	—
Copper, Cu	—	0.25	0.12
Total	100.00	100.00	100.00

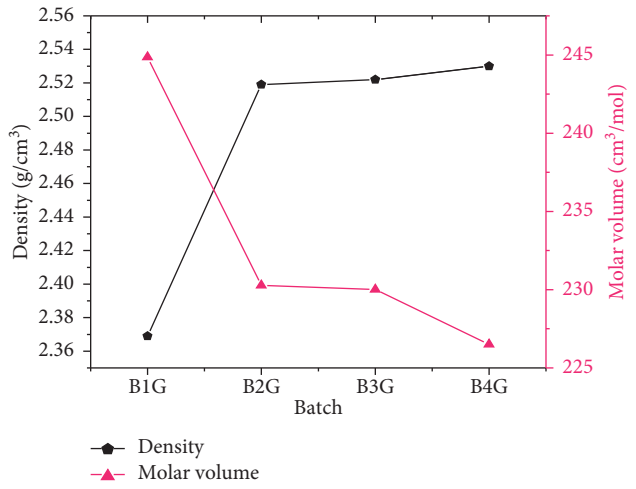

Figure 1: Graph of density and molar volume against different batches of ASF bioglass samples.

samples. The density of the ASF bioglass for B1G to B4G was 2.37 g/cm^3, 2.51 g/cm^3, 2.52 g/cm^3, and 2.53 g/cm^3, respectively. The density of the samples increased from B1G to B4G. This is due to the high addition of CaF_2 that leads to the crystalline structure. The higher the amount of CaF_2 added, the higher the density of the sample. This is because CaF_2 acts as a flux that enhances the crystallization process [34, 35]. The high crystalline structure will produce strong glass component [14] and thus provide high density of sample. Meanwhile, the molar volume of the ASF bioglass sample is inversely proportional to the density. The density and molar volume show opposite action to each other [33]. From Figure 1, the data show decrement pattern for the molar volume results for B1G to B4G. The molar volumes for 4 batches are 244.86 cm^3/mol, 230.28 cm^3/mol, 230.00 cm^3/mol, and 226.50 cm^3/mol, respectively. The higher the amount of CaF_2 added, the lower the molar volume of ASF bioglass. This is related to the change in the amorphous structured closed-pack lattices to crystalline structured closed-pack lattices due

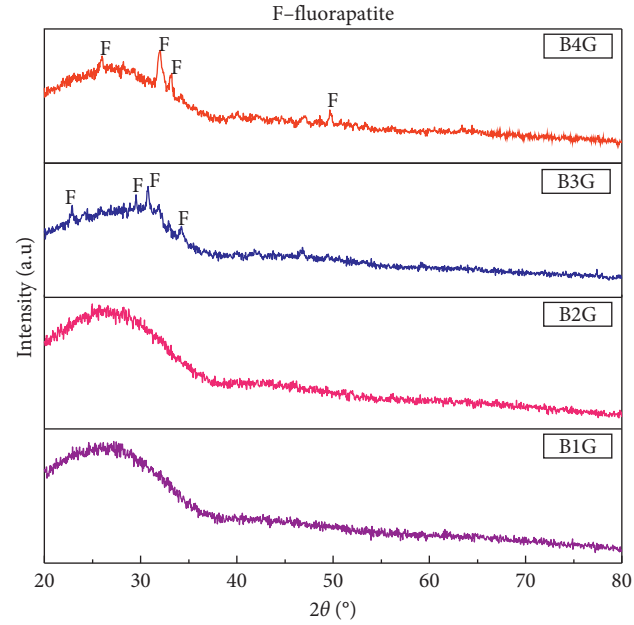

Figure 2: XRD pattern for B1G to B4G of ASF bioglass at room temperature 27°C.

Table 3: FTIR spectral band assigned to the vibrational modes.

Wavenumbers (cm^{-1})	Assignment of vibrational mode
~500	The P–O bending mode
~800	The Si–O–Si tetrahedral mode
~1300	The C–O stretching mode
~1600	The O–H stretching mode

to the presence of fluoride which acts as a nucleation agent in the glass [16]. The crystalline structure of the sample is arranged in highly ordered structure, making the sample more compact thus decreasing the molar volume of the sample. The density and molar volume are related to atomic weight, ionic size, and total amount of different elements in ASF bioglass system.

3.3. X-Ray Diffraction (XRD). The XRD patterns for various ASF bioglass samples are shown in Figure 2; B1G and B2G indicate that the ASF bioglass system is in an amorphous phase and no sharp peaks exist due to the optimum CaF_2 concentration, which acts as a stabilizer for the bioglass system [36]. However, the presence of peaks in B3G and B4G is due to the presence of initial crystalline peaks in ASF bioglass samples. The observed small and sharp peaks are known as fluorapatite ($Ca_5(PO_4)_3F$) with reference code JCPDS no. 98-001-7206. This may be due to the high fluoride content from CaF_2 in both samples [37]. Higher percentages of CaF_2 lead to crystalline structured while lower fluoride content gives amorphous structured [38]. This is because CaF_2 acts as a flux which increases the crystallization [34, 35]. In addition, fluoride enhances the nucleation and growth of crystalline phase through the incorporation of F^- ions into the ASF bioglass network where it replaces

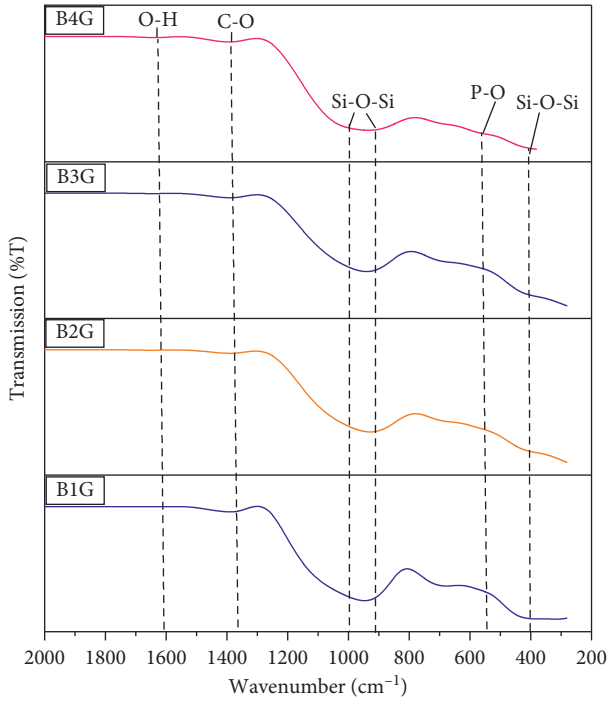

Figure 3: FTIR spectra for different batches of alumino-silica-fluoride (ASF) based bioglass.

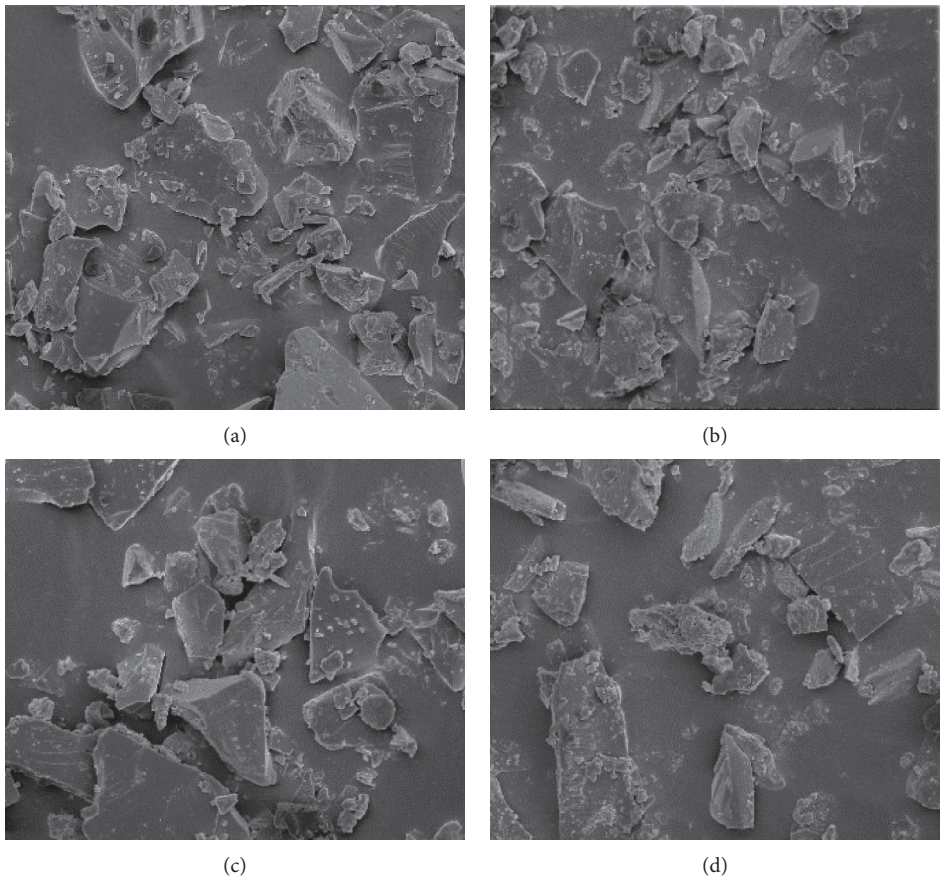

Figure 4: FESEM micrographs of glass samples at 10 000x magnification. (a) B1G. (b) B2G. (c) B3G. (d) B4G.

Element	Weight%
C K	23.25
O K	50.13
F K	1.36
Na K	1.40
Al K	7.05
Si K	6.48
P K	4.76
Ca K	5.56
Totals	100.00

Ca/P = 1.17

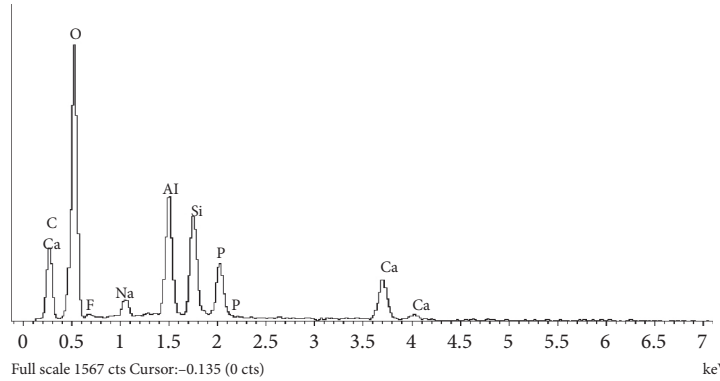

(a)

Element	Weight%
C K	19.15
O K	49.69
F K	1.16
Na K	1.77
Al K	7.18
Si K	7.83
P K	5.10
Ca K	8.13
Totals	100.00

Ca/P = 1.59

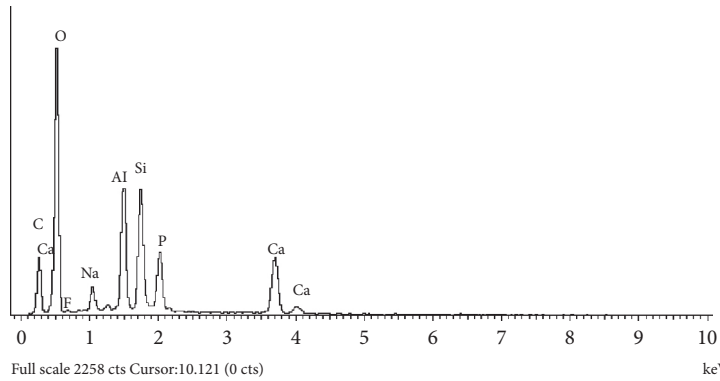

(b)

Element	Weight%
C K	18.54
O K	48.21
F K	2.12
Na K	2.29
Al K	7.27
Si K	8.26
P K	5.12
Ca K	8.19
Totals	100.00

Ca/P = 1.60

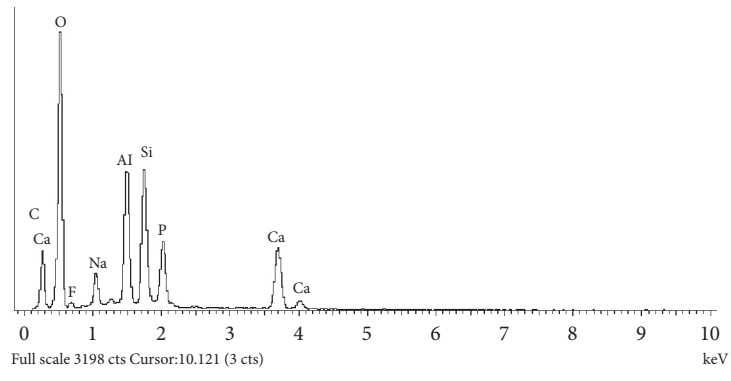

(c)

Element	Weight%
C K	18.54
O K	48.21
F K	2.12
Na K	2.29
Al K	7.27
Si K	8.26
P K	5.12
Ca K	8.19
Totals	100.00

Ca/P = 1.77

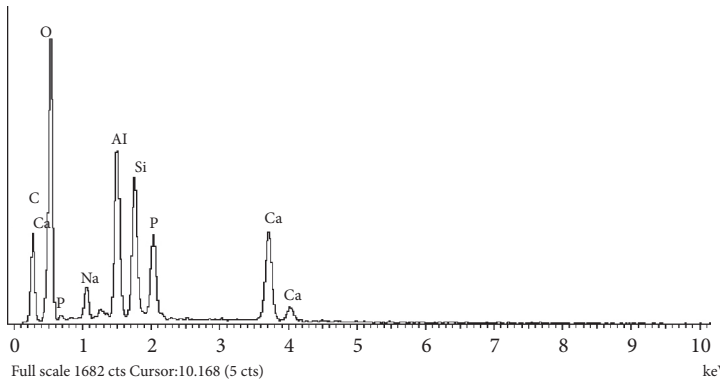

(d)

Figure 5: EDX spectra with Ca/P ratio calculation for B1G to B4G of ASF bioglass. (a) B1G. (b) B2G. (c) B3G. (d) B4G.

nonbridge oxygen ions and lowers the aggregation extent of the glass network [39–42].

3.4. Fourier Transform Infrared (FTIR). Table 3 and Figure 3 present the FTIR spectra of ASF bioglass with different weight percentages of CaF_2. Based on the figures, the major bands exist in all batches represented by the infrared (IR) spectra belong to glass modes such as Si–O–Si, P–O, and C–O mode band. However, the presence of hydroxide group existing at the range of ~1600 cm^{-1} is known as O–H stretching mode [43, 44]. The IR spectrum of all ASF bioglass samples at the range of ~400 cm^{-1} due to Si–O–Si bending [45–47]. The presence of Si–O–Si tetrahedral in the range ~800 to 1000 cm^{-1} is due to the formation of the silica-rich layers. The P–O bending mode exists at the range ~500 cm^{-1} showing the formation of calcium phosphate layers in glass sample [48, 49]. Another band spectrum exists at the range of 1300 cm^{-1} known as C–O stretching. This C–O bond exists in all batches indicating the presence of carbonate groups in CaO. The carbonate presents in the powder may be due to the dissolution of carbon dioxide (CO_2) from the atmosphere [23, 44]. The same intensity level across all bands indicates a consistent ASF Bioglass formation in all samples.

3.5. Field Emission Scanning Electron Microscopy (FESEM). Figure 4 shows FESEM micrographs of 4 batches of glass samples. The microstructure observations show nonuniform particle distribution based on the formation of irregular shapes and sharp particle edges in all glass samples [50]. The amount of CaF_2 content added does not affect the glass structure of ASF bioglass. The use of ASF bioglass in dental applications is due to the good adhesive properties and biocompatibility that make glass a potential candidate in medical procedures [7].

3.6. Energy Dispersive X-Ray Analysis (EDX). The EDX spectra for Batches 1 to 4 are shown in Figure 5 for the identification of weight percentage of C, O, F, Na, Al, Si, P, and Ca by quantitative analysis. The Ca/P ratio calculations are shown in Figure 5 for each sample. The Ca/P ratio for calcium phosphate bioglass around 1.5 and 1.67 belongs to apatite groups such as fluorapatite or hydroxyapatite [51]. The Ca/P ratio calculation for each sample increased from 1.17 to 1.77 due to an increase in the amount of CaF_2 in the ASF bioglass. The release of calcium and phosphorus ions helps in the formation of apatite layers in glass structure [37]. The high amounts of ion release will form apatite layer as the ionic activity increases during apatite nucleation process [52]. The formation of Ca and P ions is important in dental applications as it can increase the apatite saturation by enhancing the remineralization [53]. The ASF bioglass materials are chemically identical to the dental structure components. Therefore, it can help repair damaged tissues in the biological system. From the previous study of bioglass, the Ca/P values higher than 1 were suitable for the body implantations while Ca/P values lower than 1 were not appropriate for biological implants due to high solubility [30, 54]. From the figure, the Ca/P ratio of the ASF bioglass is acceptable because its ratio is within the required range.

4. Conclusions

ASF based bioglass was synthesised from SLS glass and CS waste material as a SiO_2 and CaO source using conventional melt-quenching methods. The XRF results showed that the major elements in the SLS glass and CS were Si and Ca, respectively. The density of ASF bioglass was observed to increase with increasing CaF_2 content in the composition. However, molar volume showed the opposite trend. The different physical behaviors of ASF bioglass were closely related to CaF_2 content in each composition. The XRD results revealed that B1G and B2G are in an amorphous phase and no sharp peaks exist due to the optimum CaF_2 concentration, which is a stabilizer for the bioglass system. However, presence of peaks in B3G and B4G was due to the presence of initial crystalline peaks in ASF bioglass samples. The small and sharp peaks observed were known as fluorapatite ($Ca_5(PO_4)_3F$). Meanwhile, FTIR measurements revealed the presence of various chemical bonds such as Si–O–Si, P–O, C–O, and O–H in samples showing ASF bioglass formation. The FESEM microstructure showed the nonuniform particle distribution based on the formation of irregular shapes and sharp particle edges in all glass samples. Finally, EDX analysis showed that Ca/P values obtained from 1.17 to 1.77 were appropriate for biological implantation. The ASF bioglass system provided 4 batches of samples where B1G and B2G produce clear glass structures with amorphous phases. From the observations, this was the optimum weight percentage of CaF_2 to produce ASF based bioglass. Meanwhile, B3G and B4G with high CaF_2 composition showed weak crystalline phase. In conclusion, ASF bioglass has been successfully synthesised from SLS glass and CS vitreous waste material. It is known as a high potential application in material science, medicine, and biomedical field.

Data Availability

All data used to support the findings of this study are included within the article.

Conflicts of Interest

The authors have no conflicts of interest relevant to this manuscript.

Acknowledgments

The researchers are thankful for the support of this study from the Ministry of Science, Technology and Innovation, Malaysia, and Universiti Putra Malaysia (UPM), each under the Fundamental Research Grant Scheme (5540163) and Inisiatif Putra Siswazah (IPS-9627400).

References

[1] M. D. Khalid, Z. Khurshid, M. S. Zafar, I. Farooq, R. S. Khan, and A. Najmi, "Bioactive glasses and their applications in dentistry," *Journal of The Pakistan Dental Association*, vol. 26, no. 1, pp. 32–38, 2017.

[2] F. S. Tabatabaei, R. Torres, and L. Tayebi, "Biomedical materials in dentistry," in *Applications of Biomedical Engineering in Dentistry*, pp. 3–20, Springer, Newyork, NY, USA, 2020.

[3] I. Farooq, Z. Imran, U. Farooq, A. Leghari, and H. Ali, "Bioactive glass: a material for the future," *World Journal of Dentistry*, vol. 3, no. 2, pp. 199–201, 2012.

[4] J. V. Rau, I. Antoniac, G. Cama, V. S. Komlev, and A. Ravaglioli, "Bioactive materials for bone tissue engineering," *BioMed Research International*, vol. 2016, Article ID 3741428, 3 pages, 2016.

[5] M. R. Urist and R. W. Johnson, "Calcification and ossification: IV. The healing of fractures in man under clinical conditions," *Journal of Bone and Joint Surgery*, vol. 25, no. 2, pp. 375–426, 1943.

[6] M. R. Syed, M. Khan, F. Sefat, Z. Khurshid, M. S. Zafar, and A. S. Khan, "Bioactive glass and glass fiber composite: biomedical/dental applications," in *Biomedical, Therapeutic and Clinical Applications of Bioactive Glasses*, pp. 467–495, Woodhead Publishing, Cambridge, UK, 2019.

[7] F. Baino, S. Hamzehlou, and S. Kargozar, "Bioactive glasses: where are we and where are we going?" *Journal of Functional Biomaterials*, vol. 9, no. 1, pp. 1–26, 2018.

[8] L. L. Hench, "The story of bioglass," *Journal of Materials Science: Materials in Medicine*, vol. 17, no. 11, pp. 967–978, 2006.

[9] E. Patel, P. Pradeep, P. Kumar, Y. E. Choonara, and V. Pillay, "Oroactive dental biomaterials and their use in endodontic therapy," *Journal of Biomedical Materials Research Part B: Applied Biomaterials*, vol. 108, no. 1, pp. 201–212, 2020.

[10] L. L. Hench and O. Andersson, "Bioactive Glasses," *An Introduction to Bioceramics*, pp. 49–69, World Scientific, Tuck Link, Singapore, 2013.

[11] G. Kaur, O. P. Pandey, K. Singh, D. Homa, B. Scott, and G. Pickrell, "A review of bioactive glasses: their structure, properties, fabrication and apatite formation," *Journal of Biomedical Materials Research Part A*, vol. 102, no. 1, pp. 254–274, 2014.

[12] S. I. Schmitz, B. Widholz, C. Essers et al., "Superior biocompatibility and comparable osteoinductive properties: sodium-reduced fluoride-containing bioactive glass belonging to the CaO-MgO-SiO2 system as a promising alternative to 45S5 bioactive glass," *Bioactive Materials*, vol. 5, no. 1, pp. 55–65, 2020.

[13] M. A. Abbassy, A. S. Bakry, N. I. Alshehri et al., "45S5 Bioglass paste is capable of protecting the enamel surrounding orthodontic brackets against erosive challenge," *Journal of Orthodontic Science*, vol. 8, no. 1, p. 5, 2019.

[14] W. N. W. Jusoh, K. A. Matori, M. H. M. Zaid et al., "Effect of sintering temperature on physical and structural properties of Alumino-Silicate-Fluoride glass ceramics fabricated from clam shell and soda lime silicate glass," *Results in Physics*, vol. 12, pp. 1909–1914, 2019.

[15] S. M. Rabiee, N. Nazparvar, M. Azizian, D. Vashaee, and L. Tayebi, "Effect of ion substitution on properties of bioactive glasses: a review," *Ceramics International*, vol. 41, no. 6, pp. 7241–7251, 2015.

[16] A. Al-Noaman, S. C. F. Rawlinson, and R. G. Hill, "The influence of CaF2 content on the physical properties and apatite formation of bioactive glass coatings for dental implants," *Journal of Non-Crystalline Solids*, vol. 358, no. 15, pp. 1850–1858, 2012.

[17] R. G. Hill, A. Stamboulis, and R. V. Law, "Characterisation of fluorine containing glasses by 19F, 27Al, 29Si and 31P MAS-NMR spectroscopy," *Journal of Dentistry*, vol. 34, no. 8, pp. 525–532, 2006.

[18] J. D. B. Featherstone, "Prevention and reversal of dental caries: role of low level fluoride," *Community Dentistry and Oral Epidemiology*, vol. 27, no. 1, pp. 31–40, 1999.

[19] S. Ali, I. Farooq, A. M. Al-Thobity, K. S. Al-Khalifa, K. Alhooshani, and S. Sauro, "An in-vitro evaluation of fluoride content and enamel remineralization potential of two toothpastes containing different bioactive glasses," *Bio-Medical Materials and Engineering*, vol. 30, no. 5-6, pp. 487–496, 2019.

[20] D. S. Brauer, N. Karpukhina, R. V. Law, and R. G. Hill, "Structure of fluoride-containing bioactive glasses," *Journal of Materials Chemistry*, vol. 19, no. 31, pp. 5629–5636, 2009.

[21] B. Mirhadi and B. Mehdikhani, "Effect of calcium fluoride on sintering behavior of SiO2-CaO-Na2O-MgO glass-ceramic system," *Processing and Application of Ceramics*, vol. 6, no. 3, pp. 159–164, 2012.

[22] D. P. Mukherjee and S. K. Das, "SiO2-Al2O3-CaO glass-ceramics: effects of CaF2 on crystallization, microstructure and properties," *Ceramics International*, vol. 39, no. 1, pp. 571–578, 2013.

[23] N. A. A. Rahman, K. A. Matori, M. H. M. Zaid et al., "Fabrication of Alumino-Silicate-Fluoride based bioglass derived from waste clam shell and soda lime silica glasses," *Results in Physics*, vol. 12, pp. 743–747, 2019.

[24] V. W. Francis Thoo, N. Zainuddin, K. A. Matori, and S. A. Abdullah, "Studies on the potential of waste soda lime silica glass in glass ionomer cement production," *Advances in Materials Science and Engineering*, vol. 2013, Article ID 395012, 6 pages, 2013.

[25] A. Tucci, L. Esposito, E. Rastelli, C. Palmonari, and E. Rambaldi, "Use of soda-lime scrap-glass as a fluxing agent in a porcelain stoneware tile mix," *Journal of the European Ceramic Society*, vol. 24, no. 1, pp. 83–92, 2004.

[26] C. W. Sinton and W. C. LaCourse, "Experimental survey of the chemical durability of commercial soda-lime-silicate glasses," *Materials Research Bulletin*, vol. 36, no. 13-14, pp. 2471–2479, 2001.

[27] M. Z. A. Khiri, K. A. Matori, M. H. M. Zaid et al., "Crystallization behavior of low-cost biphasic hydroxyapatite/β-tricalcium phosphate ceramic at high sintering temperatures derived from high potential calcium waste sources," *Results in Physics*, vol. 12, pp. 638–644, 2019.

[28] A. J. Awang-Hazmi, A. B. Z. Zuki, M. M. Noordin, A. Jalila, and Y. Norimah, "Mineral composition of the cockle (anadara granosa) shells of west coast of peninsular Malaysia and its potential as biomaterial for use in bone repair," *Journal of Animal and Veterinary Advances*, vol. 6, no. 5, pp. 591–594, 2007.

[29] Z. Hong, R. L. Reis, and J. F. Mano, "Preparation andin vitrocharacterization of novel bioactive glass ceramic nanoparticles," *Journal of Biomedical Materials Research Part A*, vol. 88A, no. 2, pp. 304–313, 2009.

[30] N. A. Zarifah, W. F. Lim, K. A. Matori et al., "An elucidating study on physical and structural properties of 45S5 glass at different sintering temperatures," *Journal of Non-Crystalline Solids*, vol. 412, pp. 24–29, 2015.

[31] K. A. Almasri, H. A. A. Sidek, K. A. Matori, and M. H. M. Zaid, "Effect of sintering temperature on physical, structural and optical properties of wollastonite based glass-ceramic derived from waste soda lime silica glasses," *Results in Physics*, vol. 7, pp. 2242–2247, 2017.

[32] Y. S. Ok, S.-E. Oh, M. Ahmad et al., "Effects of natural and calcined oyster shells on Cd and Pb immobilization in contaminated soils," *Environmental Earth Sciences*, vol. 61, no. 6, pp. 1301–1308, 2010.

[33] M. H. M Zaid, K. A. Matori, L. C. Wah et al., "Elastic moduli prediction and correlation in soda lime silicate glasses containing ZnO," *International Journal of Physical Sciences*, vol. 6, no. 6, pp. 1404–1410, 2011.

[34] T. M. Singh, P. Suresh, J. Sandhyarani, and J. Sravanthi, "Glass ionomer cements (GIC) in dentistry: a review," *International Journal of Plant, Animal and Environmental Sciences*, vol. 1, no. 1, pp. 26–30, 2011.

[35] L. Deng, X. Zhang, M. Zhang, and X. Jia, "Effect of CaF2 on viscosity, structure and properties of CaO-Al2O3-MgO-SiO2 slag glass ceramics," *Journal of Non-Crystalline Solids*, vol. 500, pp. 310–316, 2018.

[36] S. Hashim, H. Sidek, M. Halimah, K. Matori, W. Yusof, and M. Zaid, "The effect of remelting on the physical properties of borotellurite glass doped with manganese," *International Journal of Molecular Sciences*, vol. 14, no. 1, pp. 1022–1030, 2013.

[37] A. Bakry, M. Abbassy, H. Alharkan, S. Basuhail, K. Al-Ghamdi, and R. Hill, "A novel fluoride containing bioactive glass paste is capable of re-mineralizing early caries lesions," *Materials*, vol. 11, no. 9, p. 1636, 2018.

[38] X. Chen, X. Chen, D. S. Brauer, R. M. Wilson, R. G. Hill, and N. Karpukhina, "Novel alkali free bioactive fluorapatite glass ceramics," *Journal of Non-Crystalline Solids*, vol. 402, pp. 172–177, 2014.

[39] F. A. Shah, "Fluoride-containing bioactive glasses: glass design, structure, bioactivity, cellular interactions, and recent developments," *Materials Science and Engineering: C*, vol. 58, pp. 1279–1289, 2016.

[40] M. Galván-Ruiz, J. Hernández, L. Baños, J. Noriega-Montes, and M. E. Rodríguez-García, "Characterization of calcium carbonate, calcium oxide, and calcium hydroxide as starting point to the improvement of lime for their use in construction," *Journal of Materials in Civil Engineering*, vol. 21, no. 11, pp. 694–698, 2009.

[41] A. D. Wilson, S. Crisp, H. J. Prosser, B. G. Lewis, and S. A. Merson, "Aluminosilicate glasses for polyelectrolyte cements," *Industrial & Engineering Chemistry Product Research and Development*, vol. 19, no. 2, pp. 263–270, 1980.

[42] R.-G. Duan, K.-M. Liang, and S.-R. Gu, "The effect of additives on the crystallization of Na2O-CaO-MgO-Al2O3-SiO2-TiO2 system glasses," *Journal of Materials Processing Technology*, vol. 87, no. 1–3, pp. 192–197, 1999.

[43] L. Robinet, K. Eremin, C. Coupry, C. Hall, and N. Lacome, "Effect of organic acid vapors on the alteration of soda silicate glass," *Journal of Non-Crystalline Solids*, vol. 353, no. 16-17, pp. 1546–1559, 2007.

[44] N. Montazeri, R. Jahandideh, and E. Biazar, "Synthesis of fluorapatite–hydroxyapatite nanoparticles and toxicity investigations," *International Journal of Nanomedicine,* vol. 6, pp. 197–201, 2011.

[45] T. Himanshu, S. P. Singh, K. A. Sampath, M. Prerna, and J. Ashish, "Studies on preparation and characterization of 45S5 bioactive glass doped with $(TiO_2 + ZrO_2)$ as bioactive ceramic material," *Bioceramics Development and Applications*, vol. 6, no. 1, p. 2, 2016.

[46] T. Hamasaki, K. Eguchi, Y. Koyanagi, A. Matsumoto, T. Utsunomiya, and K. Koba, "Preparation and characterization of machinable mica glass-ceramics by the sol-gel process," *Journal of the American Ceramic Society*, vol. 71, no. 12, pp. 1120–1124, 1988.

[47] I. Kansal, A. Goel, D. U. Tulyaganov, E. R. Shaaban, M. J. Ribeiro, and J. M. F. Ferreira, "The effect of fluoride ions on the structure and crystallization kinetics of La2O3-containing diopside based oxyfluoride glasses," *Ceramics International*, vol. 35, no. 8, pp. 3489–3493, 2009.

[48] O. Peitl, E. D. Zanotto, and L. L. Hench, "Highly bioactive P_2O_5-Na_2O-CaO-SiO_2 glass-ceramics," *Journal of Non-Crystalline Solids*, vol. 292, no. 1–3, pp. 115–126, 2001.

[49] Z. Hong, E. G. Merino, R. L. Reis, and J. F. Mano, "Novel rice-shaped bioactive ceramic nanoparticles," *Advanced Engineering Materials*, vol. 11, no. 5, pp. 25–29, 2009.

[50] N. Monmaturapoj, W. Soodsawang, and S. Tanodekaew, "Enhancement effect of pre-reacted glass on strength of glass-ionomer cement," *Dental Materials Journal*, vol. 31, no. 1, pp. 125–130, 2012.

[51] N. Eliaz and N. Metoki, "Calcium phosphate bioceramics: a review of their history, structure, properties, coating technologies and biomedical applications," *Materials*, vol. 10, no. 4, p. 334, 2017.

[52] M. T. Islam, R. M. Felfel, E. A. Abou Neel, D. M. Grant, I. Ahmed, and K. M. Z. Hossain, "Bioactive calcium phosphate–based glasses and ceramics and their biomedical applications: a review," *Journal of Tissue Engineering*, vol. 8, Article ID 204173141771917, 2017.

[53] M. Iafisco, L. Degli Esposti, G. B. Ramírez-Rodríguez et al., "Fluoride-doped amorphous calcium phosphate nanoparticles as a promising biomimetic material for dental remineralization," *Scientific Reports*, vol. 8, no. 1, p. 17016, 2018.

[54] S. M. Best, A. E. Porter, E. S. Thian, and J. Huang, "Bioceramics: past, present and for the future," *Journal of the European Ceramic Society*, vol. 28, no. 7, pp. 1319–1327, 2008.